

Supporting Information

3D printing of layered vanadium disulfide for water-in-salt electrolyte- zinc-ion batteries

Stefano Tagliaferri,^a Goli Nagaraju,^a Maria Sokolikova,^a Rachael Quintin-Baxendale,^a Cecilia Mattevi^a*

^a Department of Materials, Imperial College London, London SW7 2AZ, United Kingdom

*Corresponding author: c.mattevi@imperial.ac.uk

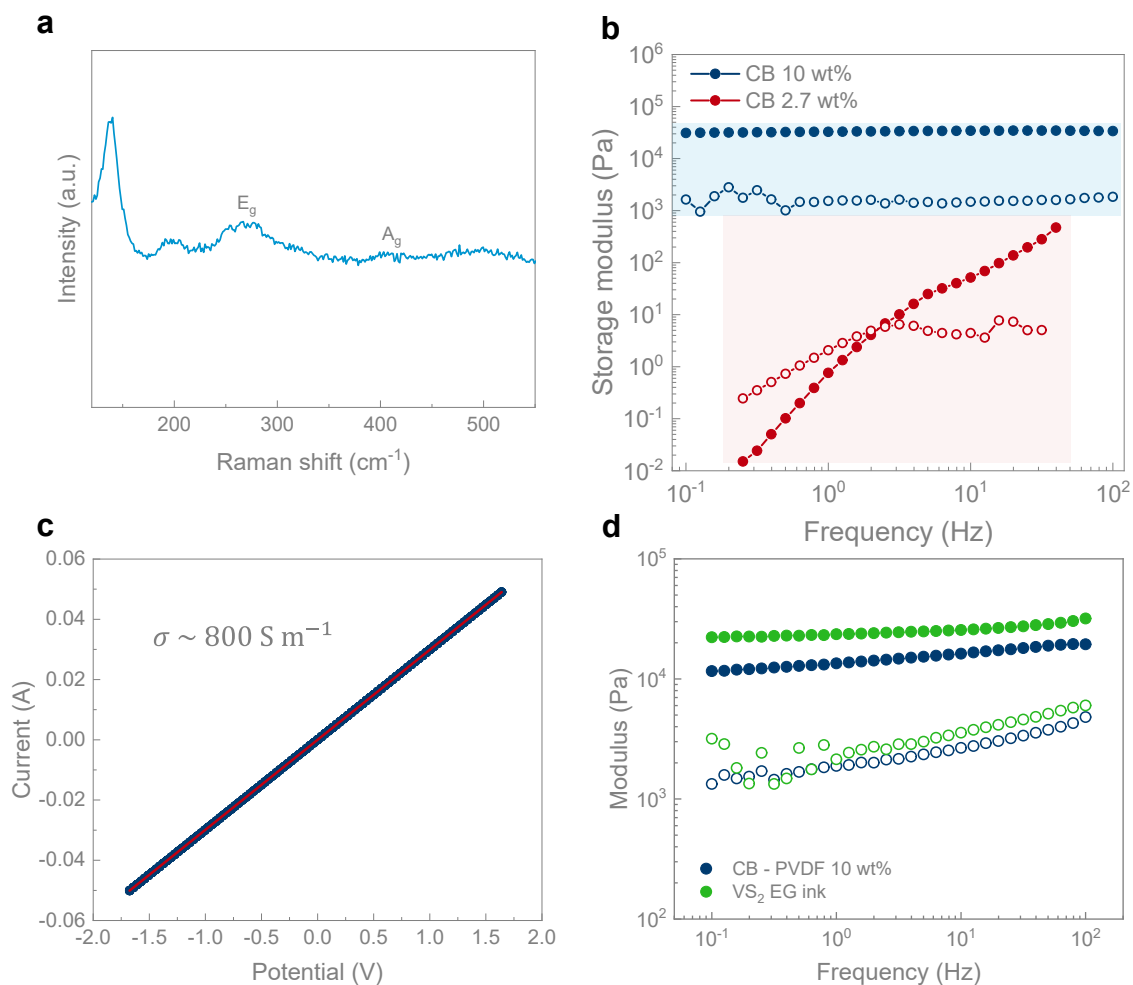
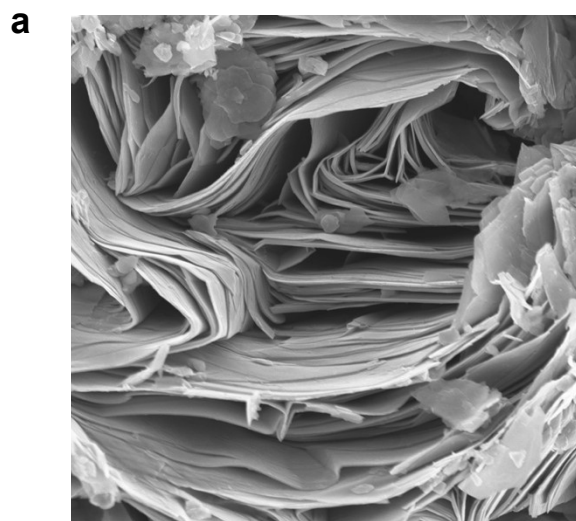
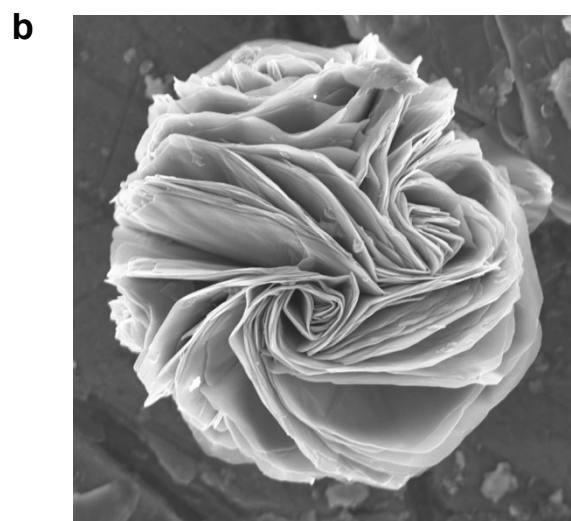


Figure S1: a) Raman spectrum of hydrothermal VS_2 ; b) oscillatory rheology (frequency sweep) of carbon black dispersions in DMSO at different concentrations; c) I-V curve for the carbon black – PVDF conductive paste, presenting a conductivity of 800 S m^{-1} ; d) oscillatory rheology (frequency sweep) of the carbon black – PVDF ink and the VS_2 ink showing a gel-like behaviour.



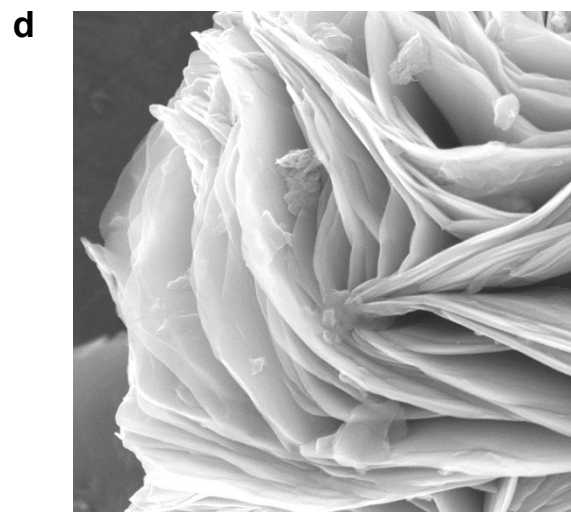
— 1 μm



— 1 μm



— 500 nm



— 500 nm

Figure S2: SEM images of hydrothermal VS_2 synthesized a,c) in water with no ethylene glycol, c,d) in water with ethylene glycol

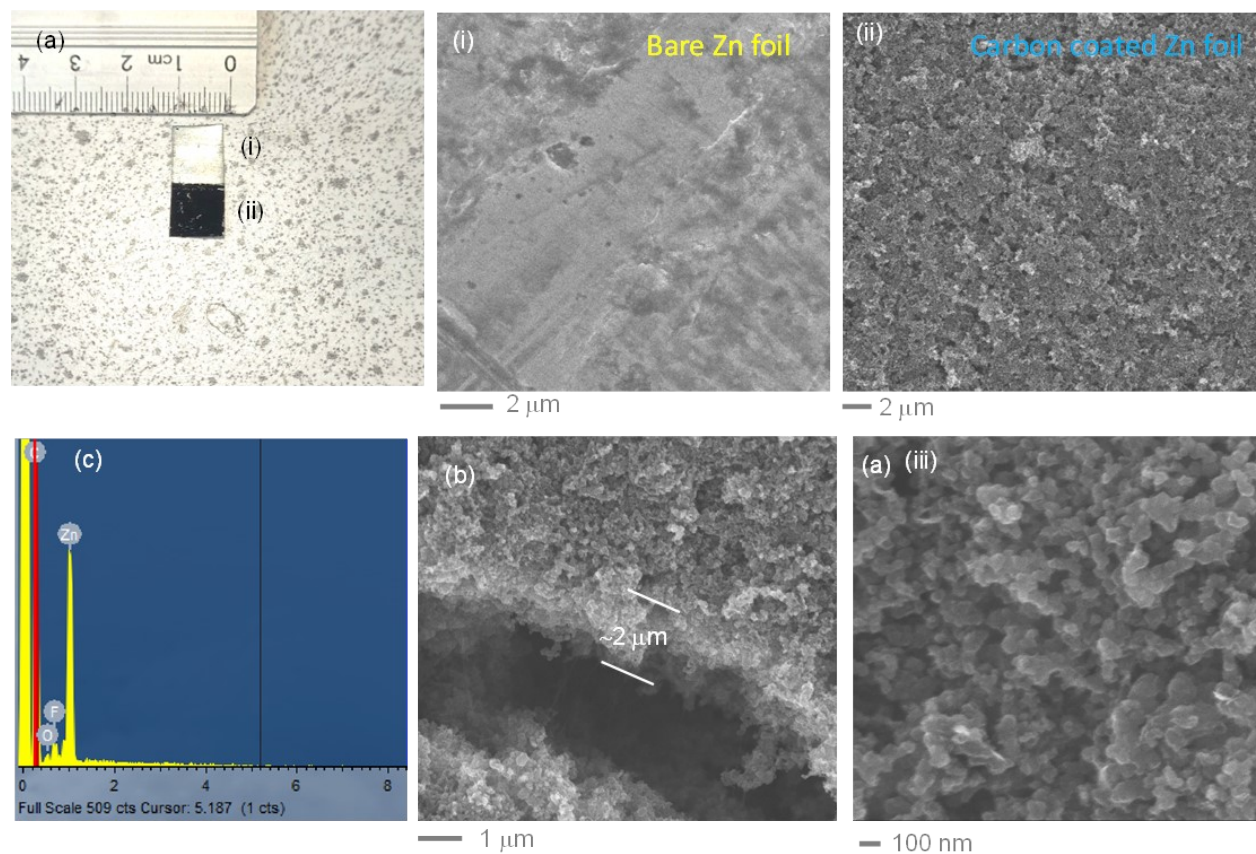


Figure S3: a) photographic image and a(i-iii) Low- and high-magnification SEM images of printed C@Zn foil anode using doctor blade method. SEM images demonstrate that the noncarbon is randomly distributed on the Zn foil with a thickness of $\sim 2 \mu\text{m}$ (b), while the bare Zn foil (i) showing smooth surface. b) Thickness of the printed carbon on Zn foil. The elemental distribution of C@Zn foil was measured using EDX spectrum (c), which shows the characteristic peaks of C, Zn and F elements related to the carbon black, PVdF binder and Zn metal foil.

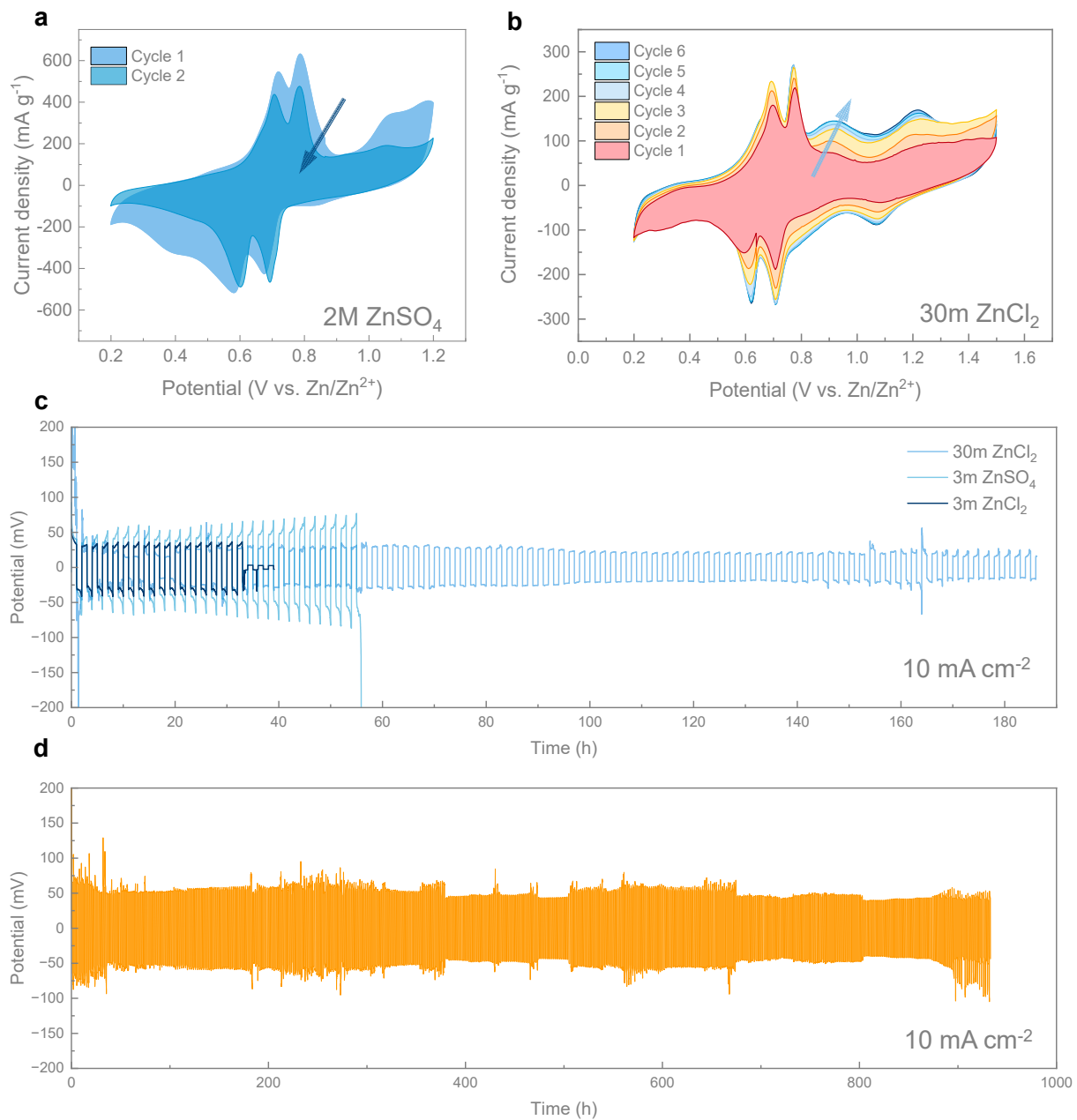


Figure S4: Comparison of the cyclic voltammograms of hydrothermal VS_2 in a) 2M ZnSO_4 and b) 30 m ZnCl_2 ; c) galvanostatic plating/stripping tests (10 mA cm^{-2}) conducted on symmetric zinc foil cells in different electrolytes; d) galvanostatic plating/stripping tests (10 mA cm^{-2}) conducted on symmetric zinc foil coated with carbon black in 30m ZnCl_2 .

Peak 1	0.47	Peak 4	0.48
Peak 2	0.43	Peak 5	0.49
Peak 3	0.73	Peak 6	0.74

Table S1:
Results

of the kinetic analysis on the VS₂ electrodes

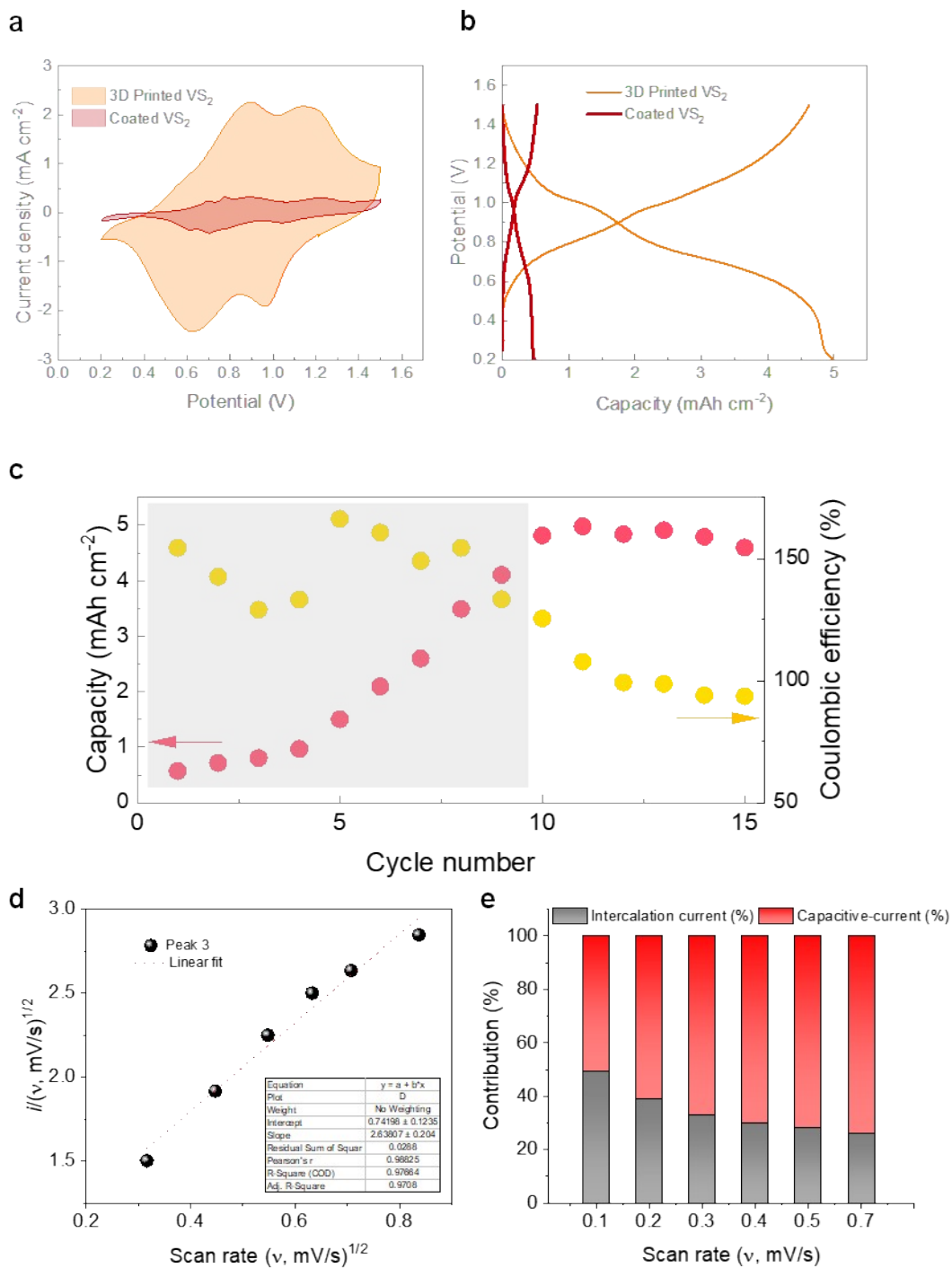


Figure S5: a) Cyclic voltammetry of the 3D printed VS₂ cathode and slurry-coated VS₂ cathode; b) galvanostatic charge-discharge of the 3D printed VS₂ cathode and slurry-coated VS₂ cathode (0.2 mA cm⁻²); c) capacity retention and coulombic efficiency of the 3D printed VS₂ cathode (0.2 mA cm⁻²). (d)

relationship of squar root of scan rate ($v, \text{mv s}^{-1}$)^{1/2} vs. $i/(v, \text{mv s}^{-1})^{1/2}$ and e) capacitive- and diffusion-controlled current contribution of the VS₂-based ZIB.

The capacitive-type and diffusion-type current contribution of VS₂-based ZIBs were quantified using the modified Power-law, as shown below. This evidences that the peak current (i_p) is related to the combination of capacitive-controlled (S_1v) and diffusion-controlled (S_2v) processes.^{1, 2}

$$i_p = S_1v + S_2v^{1/2} \quad (1)$$

$$i_p/v^{1/2} = S_1v^{1/2} + S_2v \quad (2)$$

Here, i_p , v , S_1 , and S_2 indicate the peak current, scan rate, and constants, respectively. By plotting the linear fit of $i/v^{1/2}$ vs. $v^{1/2}$, as shown in the Figure S5d, the slope and intercept values of S_1 and S_2 can be obtained. Thus, the portion of capacitive- and diffusion-controlled contributions during the redox process were calculated using Eq. (2) and plotted in Figure S5(e). At a low-scan rate of 0.1 mV s⁻¹, the VS₂ showed intercalation current contribution of 49.4% with a capacitive- contribution of 50.6%). While at the higher scan rate (0.7 mV s⁻¹), capacitive-type current contribution was enhanced to 73.9% owing to the surface oxidation of VS₂. These results collectively verify the mixed charge storage behaviour of the VS₂ with ZnCl₂ electrolyte.

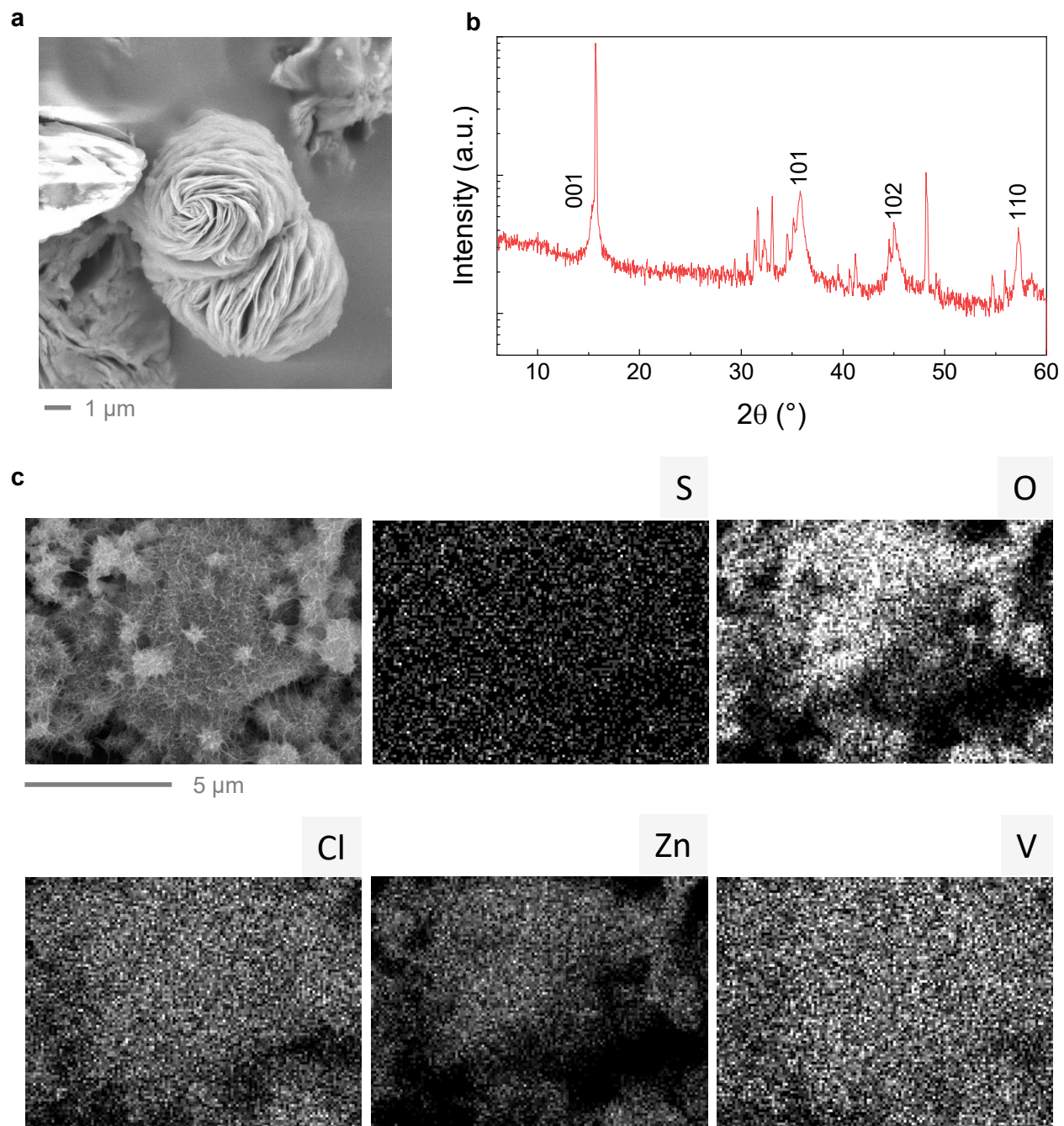


Figure S6: a) SEM imaging of the VS₂ nanoflowers after soaking in WISE for 14 days; b) XRD on the VS₂ nanoflowers soaked in WISE for 14 days, with the reflections originating from VS₂ (labelled peaks); the other peaks likely arise from unwashed WISE and corresponding by-products (*e.g.* zinc hydroxychlorides); c) EDS mapping of the VS₂ nanoflowers after soaking in WISE for 14 days.

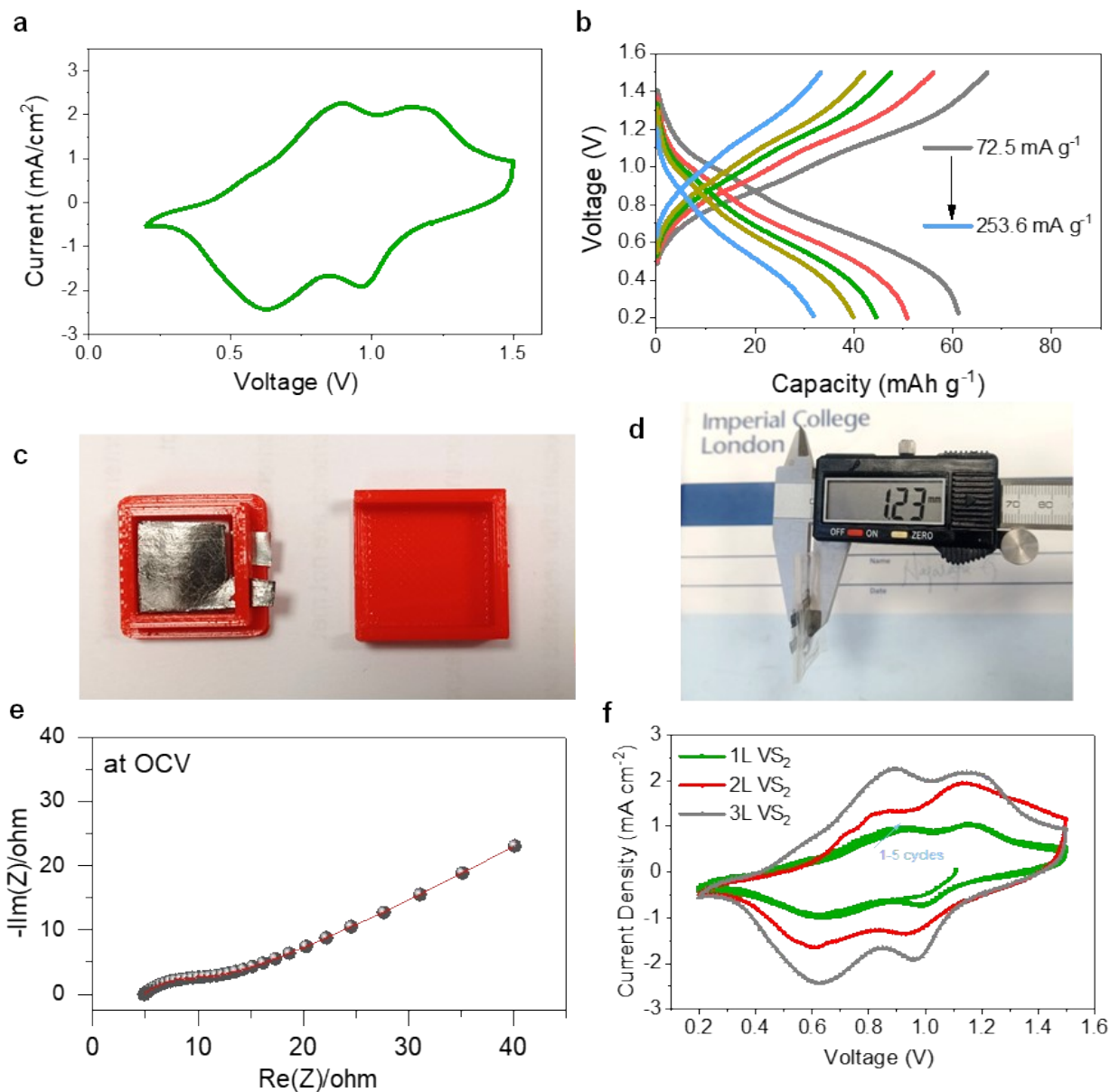
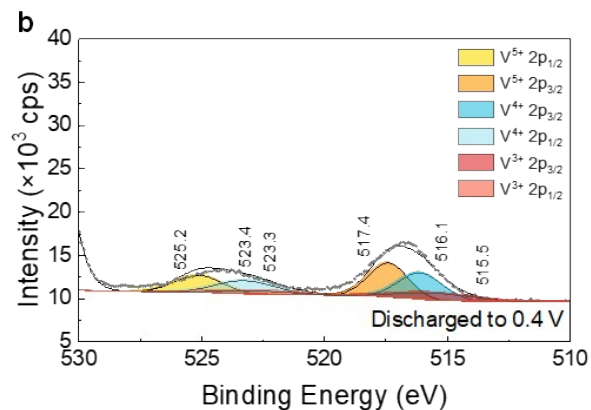
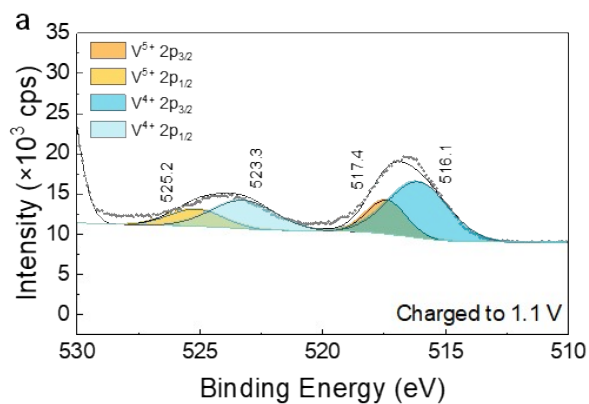


Figure S7: a) Cyclic voltammety of the 3D printed 3L VS₂/C@Zn cell components, after soaking in WISE for 14 days (0.2 mV s⁻¹); b) gravimetric charge-discharge curves of the ZIB with a 3D printed 3L VS₂ cathode; c) digital photographs showing the encapsulation of the substrate with the printed electrode inside a 3D printed polylactic acid case and d) thickness of the pouch-type ZIB using 3L VS₂ and C@Zn electrodes with 30m ZnCl₂ electrolyte. e) Nyquist plot of 3L VS₂/C@Zn cell at open circuit voltage (OCV) and f) cyclic voltammety curves showing the effect of 3D printing layers (1-3 layers of VS₂) on redox performance of ZIBs.



c

	Peak BE	Atomic %
V^{5+}	517.4	28.8
V^{4+}	516.1	71.2

d

	Peak BE	Atomic %
V^{5+}	517.4	42.8
V^{4+}	516.1	37.9
V^{3+}	515.5	19.3

Figure S8: high-resolution XPS spectra of the V 2p core-level electrons during charge (a) and discharge (b), and corresponding atomic compositions (c, d).

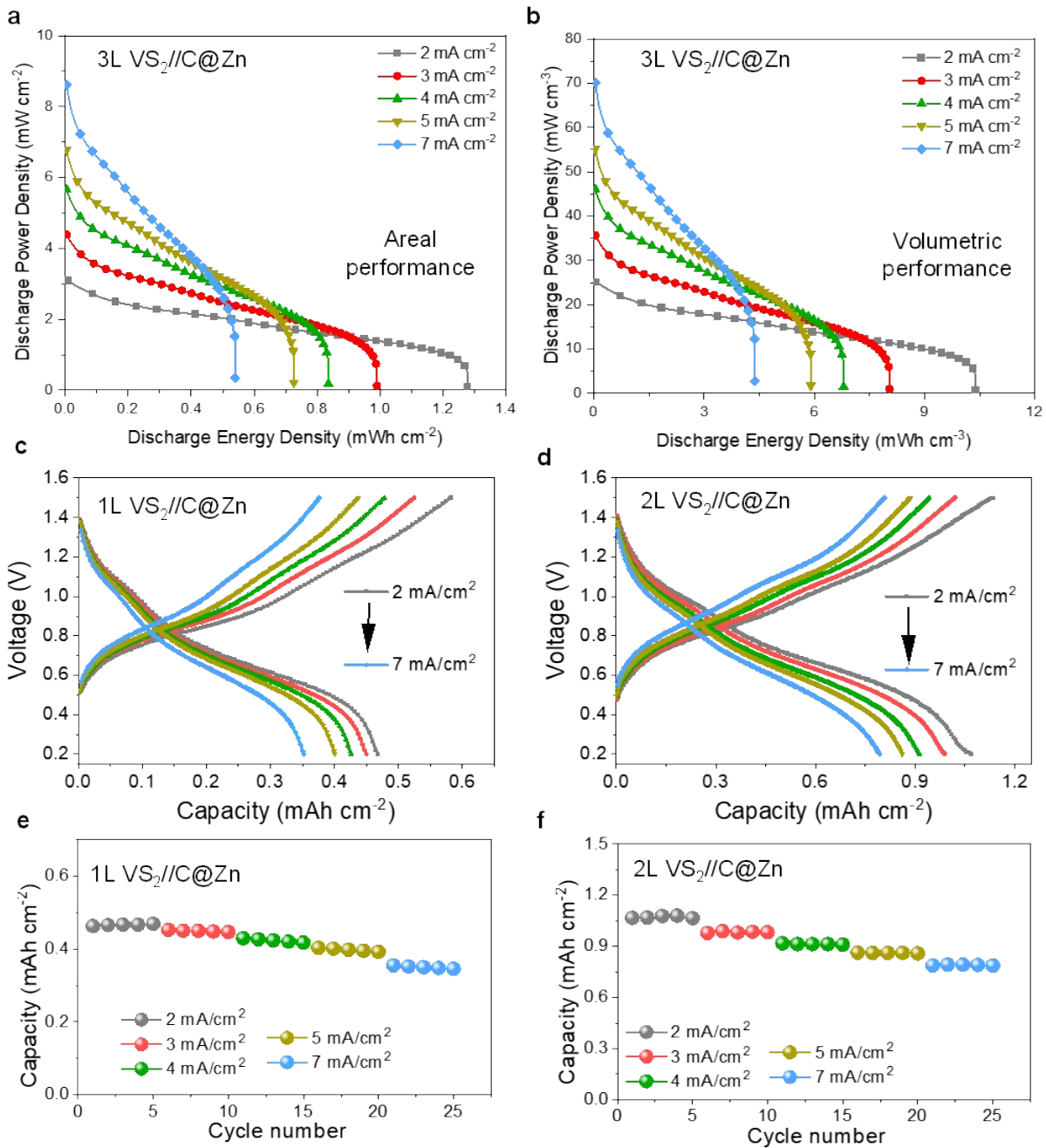


Figure S9. Discharge energy density vs. power density of fabricated of 3L VS₂//C@Zn cell measured under various current densities of 2-7 mA cm⁻². a) Areal performance and b) volumetric performance. c)-f) charge-discharge capacity profiles and rate capability vs. cycle number of 1L VS₂//C@Zn and 2L VS₂//C@Zn cells.

SI References:

1. Junlin Lu, Hao Ran, Jien Li, Jing Wan, Congcong Wang, Peiyuan Ji, Xue Wang, Guanlin Liu, Chenguo Hu. A fast composite-hydroxide-mediated approach for synthesis of 2D-LiCoO₂ for high performance asymmetric supercapacitor. *Electrochimica Acta*, 331, 135426, (2020).
2. Yuhang Dai, Chengyi Zhang, Jianwei Li, Xuan Gao, Ping Hu, Chumei Ye, Hongzhen He, Jiexin Zhu, Wei Zhang, Ruwei Chen, Wei Zong, Fei Guo, Ivan P. Parkin, Dan J. L. Brett, Paul R. Shearing, Liqiang Mai, Guanjie He. Inhibition of Vanadium Cathodes Dissolution in Aqueous Zn-Ion Batteries. *Adv. Mater.* 2310645 (2024).